Materials Science Research International, Vol.5, No.1 pp.45-50 (1999)

General paper

CHANGE IN RESIDUAL STRESSES OF TiN FILMS DUE TO ANNEALING TREATMENTS

Tatsuya MATSUE*, Takao HANABUSA** and Yasukazu IKEUCHI*

*Niihama National College of Technology
7-1 Yagumo-cho Niihama 792-8580, Japan
**Faculty of Engineering, Tokushima University
2-1 Jyosanjima-cho Tokushima 770-8506, Japan

Abstract: The structure and residual stresses of TiN films deposited on a steel substrate were investigated by X-ray diffraction. TiN films approximately 4 μm thick were deposited on one side of the substrate by thermal chemical vapor deposition (TiN_{CVD} film). The TiN_{CVD} film exhibited high {100} orientation. The two-exposure method was used to evaluate residual stresses in the TiN films by measuring lattice strains in the directions determined by the crystal orientation of the film. The TiN_{CVD} films had the compressive residual stress of -1.8 GPa, which is as large as the thermal residual stress expected from a thermal strain mismatch between the film and the substrate. The residual stresses did not change by annealing at temperatures below 1073 K, but they increased with increasing annealing temperatures above 1073 K, almost along with the thermal residual stresses. By X-ray photoelectron spectroscopy (XPS), we determined the ratio of nitrogen to titanium (N/Ti) after the annealing treatments. The results of the XPS analysis showed that the initial value of N/Ti was about 1.08 in the as-deposited TiN films and that the ratio of N/Ti did not change after annealing at temperatures below 1073 K, but decreased to 1.00 after annealing at temperatures above 1073 K.

Key words: *Titanium nitride, Chemical vapor deposition, X-ray diffraction, X-ray photoelectron spectroscopy, Residual stress, Annealing treatment*

1. INTRODUCTION

TiN coatings are widely used as a thermal corrosion barrier and a wear resistance. They are usually deposited on steel, e.g. on punching dies and cutting tools, to extend their lives. However, large residual stresses are necessarily enervated in coating films due to mismatch of thermal expansion between the film and the substrate and other reasons [1-3], exerting a great influence on the mechanical properties of coated material. Therefore, it is important to know the state of residual stresses in the film and the substrate.

X-ray stress measurement is very useful to investigate these residual stresses in the coatings. Considerable efforts [4, 5] have been made in stress measurement of various ceramic coatings (including TiN), deepening our understanding about the relationship between the residual stress and process parameters such as depositing temperatures.

In the previous paper [6], we found that the residual stresses in the TiN films deposited by the Multi-Arc physical vapor deposition method (TiN_{PVD} film) were changed by annealing. In the present paper, we investigate the stress state in the TiN films deposited by thermal chemical vapor deposition (TiN_{CVD} film) based on the X-ray stress measuring method. By X-ray photoelectron spectroscopy (XPS), we determined the ratio of nitrogen to titanium (N/Ti) after the annealing. A comparison was made between the residual stresses in the TiN_{CVD} and TiN_{PVD} films and the ratio of N/Ti after annealing.

2. EXPERIMENTAL DETAILS

2.1. Materials

Spring steel (SUP3:JIS) plates measuring 12 mm × 20 mm × 4 mm was used as a substrate. Before deposition the substrate was ground to the surface roughness of 0.05 μm *Ra*, and then annealed for 1 hour at 873 K. Residual stresses of the annealed substrate were ranging from -5 MPa to 10 MPa.

TiN_{CVD} and TiN_{PVD} films were deposited on one side of the substrate by thermal CVD and Multi Arc

Table 1. Conditions of TiN depositing.

Name of specimen	Film	Film thickness μm	Depositing temperature K	Coating method
TiN_{PVD}	TiN	4	523	PVD
TiN_{CVD}			973	CVD

Received August 7, 1998
Accepted January 14, 1999

PVD. The films was approximately 4 μm in thickness. Table 1 shows conditions of TiN depositing.

2.2. X-ray Stress Measuring Method

As it will be explained in detail in the following, the TiN_{CVD} and TiN_{PVD} films exhibit high {100} and {111} orientation, respectively. In such a case, no diffraction intensity appears at any ψ angle except for particular angles ψ defined by the crystal structure combined with crystal orientation. Because the $\sin^2\psi$ method cannot be adopted in this case, residual stresses in the TiN films were evaluated by the two-exposure method with measuring lattice strains in the directions determined by the crystal orientation of the film [6]. When {100} plane of the cubic lattice lies parallel to the surface, TiN420 diffraction appears at $\psi_1 = 26.6^\circ$ and $\psi_2 = 63.4^\circ$. When the {111} plane of the cubic lattice lies parallel to the surface, we obtain 222 diffractions at $\psi = 0^\circ$ and 70.5° [6,7]. In the both cases, ψ is the angle between the normal of the specimen surface and the normal of the diffraction plane. In this case, if we assume an equal-axial plane stress state, the following equation can be used for evaluating residual stress σ,

$$\sigma = \frac{E}{1+\nu} \cdot \frac{d_{\psi 1} - d_{\psi 2}}{d_0} \cdot \frac{1}{\sin^2\psi_1 - \sin^2\psi_2}, \quad (1)$$

where E and ν are Young's modulus (429 GPa) and Poisson's ratio (0.19) respectively, these have been calculated from the single-crystal elastic constants of TiN by using the Eshelby-Kröner model [8]. d_0 is the spacing of the same planes in the absence of stress. $d_{\psi 1}$ and $d_{\psi 2}$ are the strains calculated by the Bragg low from the 2θ values of TiN420 and TiN222 diffraction at the above two ψ angles. Table 2 shows X-ray measurement conditions.

2.3. X-ray Photoelectron Spectroscopy(XPS) Analysis

The ratio of N/Ti was determined by X-ray photoelectron spectroscopy (XPS) depth profile analysis of Perkin Elmer Phi 1600E [Mgkα]. The XPS analysis was performed after Ar sputter etching on TiN film surface.

The depth profile of the spectra of N-1*s* and that of Ti-2*p* peaks were measured by the XPS analysis. We calculated the ratio of N/Ti by comparing the areas of N-1*s* peak with that of Ti-2*p* peak after background corrections.

2.4. Annealing Treatment

In order to investigate how the structure and the residual stress in the film change by heat-cool cycles, the specimens were annealed in a vacuum furnace at temperatures of 473, 673, 873, 1073, 1273 and 1473 K. The duration of each temperature was 60 minutes. After annealing treatment, specimens were cooled down to the room temperature.

Table 2. X-ray measurement conditions.

Material	TiN
Characteristic X-ray	CuKα
Tube voltage	40kV
Tube current	20 mA
X-ray optics	Para-forcusing
Filter	Nickel
Diffraction for stress mesurement (2θ,deg.)	TiN420(CVD) (108.7) TiN222(PVD) (78)
Irradiated area	$2 \times 8mm^2$

3. EXPERIMENTAL RESULTS

3.1. Crystal Orientation of TiN Film

Figure 1 shows examples of the X-ray diffraction pattern from the TiN_{CVD} film. Because of the high {100} orientation of the TiN_{CVD} film, only two intensity peaks, 200 and 400 diffraction of TiN_{CVD}, were detected in θ-2θ scanning for both as-deposited and annealed TiN_{CVD} films. The peak intensity of 200 and 400 diffraction did not change by annealing below 1073 K. However, many diffraction peaks including 200 and 400 diffraction appeared after annealing at 1273 K. The intensity of all these peaks from the TiN film decreased

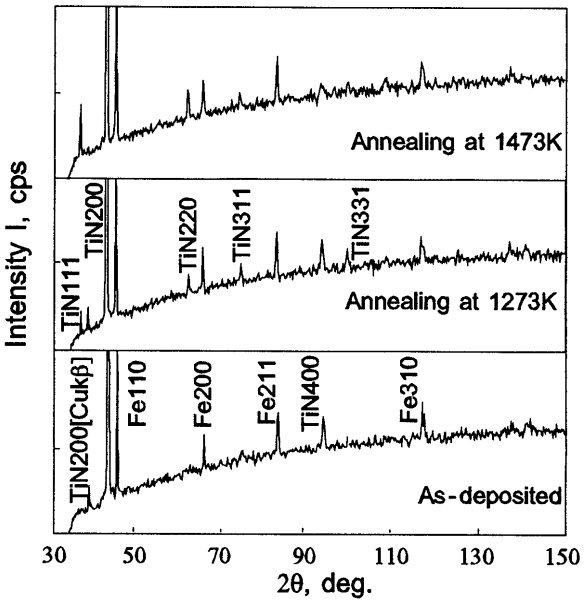

Fig.1. Change in diffraction pattern of TiN_{CVD} film with annealing treatment; as-deposited and after annealing at 1273 K and 1473 K.

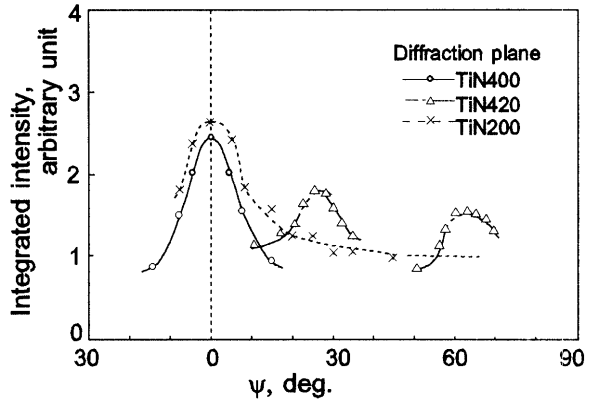

Fig.2. Integrated intensity distribution against ψ; as-deposited TiN_{CVD} film, TiN200, 400 and 420 diffractions, CuKα radiation.

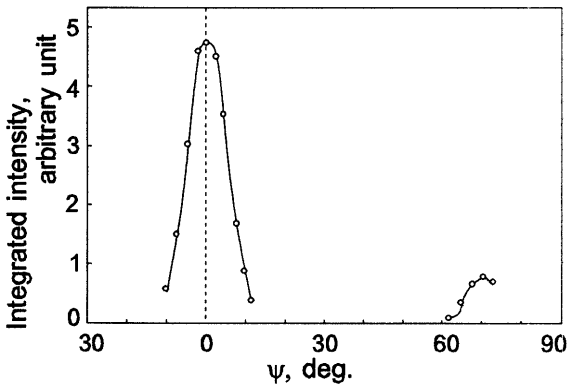

Fig.3. Integrated intensity distribution against ψ angles; TiN 222 diffraction, as-deposited TiN_{PVD} film, CuKα radiation.

after annealing at 1473 K.

When {100} plane of the cubic lattice lies parallel to the surface, TiN420 diffraction appears at $\psi = 26.6^{\circ}$ and 63.4°. Figure 2 shows the distribution of integrated intensity in the TiN_{CVD} film at ψ-angles. TiN400 diffraction and TiN420 diffraction appeared within a few degrees around $\psi = 0^{\circ}$, 27° and 63°, respectively. The TiN200 shows a peak around $\psi = 0^{\circ}$ and a gentle decrease at ψ-angles, i.e., small TiN200 diffraction appeared even after a large increase in ψ. These results mean that the TiN_{CVD} film is mainly composed of {100} oriented crystal, i.e., the {100} crystal axis of the TiN crystals coincides with the normal of the TiN film surface, but small parts of the crystal are randomly oriented.

On the other hand, in the case of TiN_{PVD} film, only two intensity peaks of 111 and 222 diffractions of TiN were detected by 2θ scanning for both the as-deposited TiN_{PVD} film and the annealed TiN_{PVD} film. Figure 3 shows the integrated intensity distribution against ψ angles in the TiN_{PVD} film. The {111} of TiN crystals

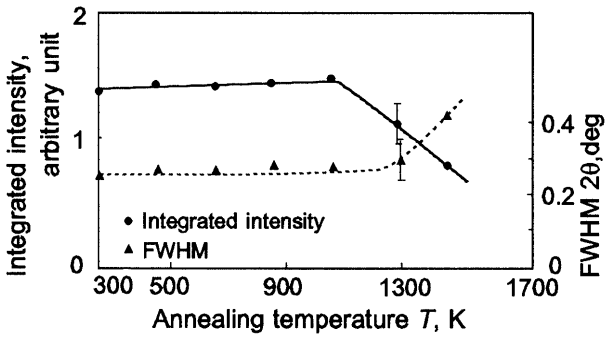

Fig.4. Changes in integrated intensity and FWHM with increasing annealing temperatures, TiN_{CVD} film, TiN200 diffraction.

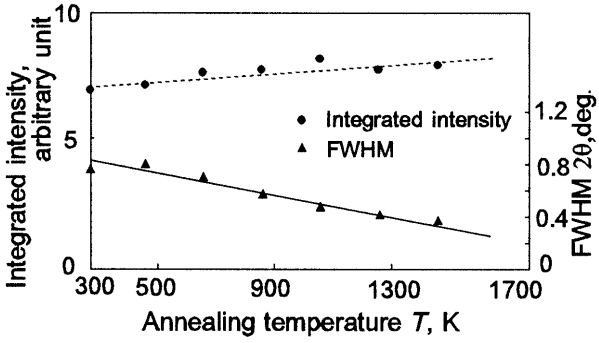

Fig.5. Change in integrated intensities and FWHM with increasing annealing temperature TiN_{PVD} film, TiN200 diffraction [6].

orients parallel to the surface normal of the substrate within ± 10 degrees. These results mean that the TiN_{PVD} film exhibited high {111} orientation.

3.2. Change in Crystal Structure of TiN Film

Figure 4 represents the changes in integrated intensity and in the full width at half-maximum intensity (FWHM) by annealing in the TiN_{CVD} film. These data were obtained from TiN200 diffraction at $\psi = 0^{\circ}$. Each of the points in the figure shows the average value of measurements of five times. For annealing at 1273 K, the measured values scatter largely as shown by the error bar, which represents the range of the measured values. For the other annealing, the scatter was below one order of magnitude. The integrated intensity and the FWHM did not change by annealing below 1073 K. However, a large decrease in the integrated intensity and a large increase in the FWHM were observed after the annealing above 1073 K.

Figure 5 was obtained from 222 diffraction of TiN_{PVD} film. A small increase in the integrated intensity and a relatively large decrease in the FWHM were

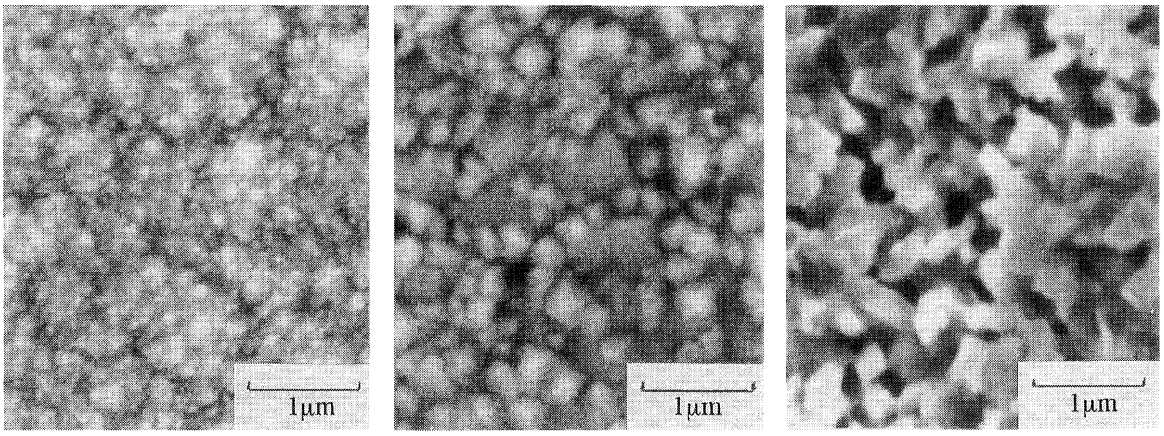

(a) as-deposited (b) 1073 K (c) 1473 K

Fig.6. Morphological change of TiN_{CVD} films with increasing annealing temperatures.

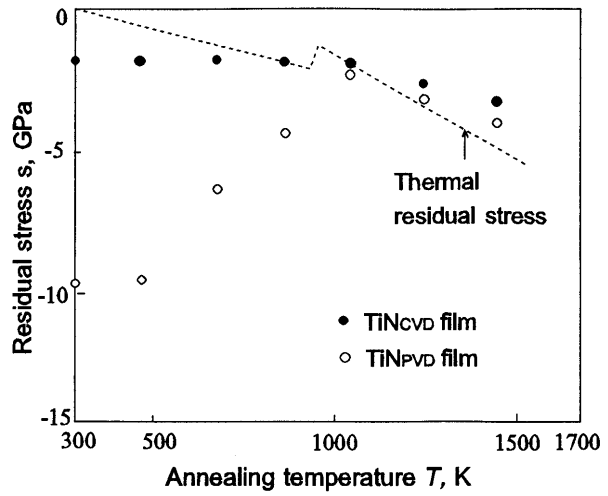

Fig.7. Changes in residual stress in the TiN_{CVD} and the TiN_{PVD} film with increasing annealing temperatures.

obtained with increasing annealing temperature. The annealing treatment caused little increase in integrated intensity of the TiN films. The increase was so small that it is thought that the TiN crystals underwent no recrystallization. A relatively large decrease in the FWHM was obtained with increasing annealing treatment. As a result, a decrease in the third kind of residual stress or growth of TiN crystal grains occurred in the film.

The annealing treatment affects the surface condition of TiN_{CVD} films. Scanning electron micrographs of the TiN_{CVD} film surfaces are shown in Fig.6. Many small TiN crystal grains were observed on the TiN film surface. They show no significant change by annealing below 873 K. Recrystallization of TiN grains appeared on the surface when the specimen was annealed at 1073 K, which was higher than the deposited temperature (973 K). After annealing at 1473 K, the growth of the recrystallized structure was observed in the film. As a result of this recrystallization, the surface roughness of the TiN_{CVD} films was increased by crystal grain growth.

3.3. Residual Stress

Figure 7 shows the residual stresses measured in the TiN_{CVD} film as well as in the TiN_{PVD} film. Residual stress of the TiN film measured for five times. The thermal residual stresses calculated from the differences in the thermal contraction of the TiN film and the substrate [6] are also plotted.

The as-deposited TiN_{CVD} and TiN_{PVD} films have high compressive residual stresses of about -1.8 and -9.8 GPa, respectively. We measured residual stresses five times. The range of the measured values was within $\pm$ 5% of the average value. The residual stresses in the TiN_{CVD} films did not change after annealing at temperatures below 1073 K. On the other hand, those in the TiN_{PVD} films decreased along with increasing annealing temperatures above 473 K, reaching the thermal residual stress level above 1073 K. The compressive residual stresses in TiN_{CVD} and TiN_{PVD} films increased by annealing above 1073 K.

4. DISCUSSION

4.1. Effect of Thermal Residual Stress

The development of the residual stress in the film depends on the deposition conditions, such as temperature, ion bombardment (in PVD method) and environment. Mismatched thermal contraction between the film and the substrate generates thermal residual stress after cooling from the depositing temperature to room temperature. Assuming that there is no stress at the depositing temperature, the thermal residual stress is given by

$$\sigma_{th} = \frac{E_F}{1-\nu_F} \{(\alpha_F - \alpha_{sub}) \Delta T + \Delta \varepsilon\}, \qquad (2)$$

where E_F and ν_F are, respectively, Young's modulus and

Poisson's ratio of the film. α_F (α_F = 9.6×10^{-6} K^{-1}) is the coefficient of thermal expansion (CTE) of the film. The E_F , ν_F and α_F values are assumed to be constant. When the substrate is carbon steel, the α_{sub} changes with temperature, and the volume changes owing to the phase transformation from austenite to ferrite. The cooling process of the substrate material is divided into three regions, i.e. ①ferrite($\alpha_{sub①}$= 13.9×10^{-6} K^{-1}, below 950 K), ②transforming($\Delta\varepsilon$ = 1.54×10^{-3}, between ①and③) and ③austenite($\alpha_{sub③}$=22.4×10^{-6} K^{-1}, above 1000 K) regions. From an expansion of Eq.(2), the thermal residual stress is represented [6]. And ΔT is the temperature drop from the depositing temperature to room temperature.

The as-deposited TiN_{CVD} and TiN_{PVD} films have high compressive residual stresses of about -1.8 and about -9.8 GPa, respectively. The stress value in the TiN_{CVD} was the same as the thermal residual stress (-1.6 GPa) calculated by Eq.(2) using ΔT=700 K which is derived from the depositing temperature of 973 K. On the other hand, compressive residual stress in the TiN_{PVD} film is one order larger than the thermal residual stress (-0.57 GPa). High compressive stresses in the TiN_{PVD} films seem to have been generated not only by the stress calculated by Eq.(2) but also by an ion bombardment of the film surface during the depositing process. However, the thermal CVD method has no effect on atomic peening during the depositing process because the films grow by chemical reaction in the heating chamber where the film and substrate temperatures are equal to the depositing temperature. It appears, therefore, the residual stress in the TiN_{CVD} film originates solely from the thermal residual stress and can be calculated by the Eq.(2).

Residual stress in the TiN_{CVD} film did not change by annealing up to 1073K, but increased along the thermal residual stress after annealing above 1073K. On the other hand, residual stress in the TiN_{PVD} film decreased with increasing annealing temperatures above 473 K. After reaching the minimum value at 1073 K, it increased with increasing annealing temperatures.

4.2. The Relationship Between the Ratio of N/Ti and the Annealing Treatment

Figure 8 shows the changes in the ratio of nitrogen to titanium (N/Ti) in TiN_{CVD} and TiN_{PVD} films. By X-ray photoelectron spectroscopy (XPS), we determined the ratio N/Ti after the annealing at various temperatures. The results of the XPS analysis showed that the initial value of N/Ti was about 1.08 in as-deposited TiN_{CVD} films. The ratio of N/Ti did not change by annealing below 1073 K, but it decreased to 1.00 by annealing above 1073 K. On the other hand, the ratio of N/Ti in the TiN_{PVD} films kept its initial value (1.08) until annealing up to 1273 K, followed by a decrease to

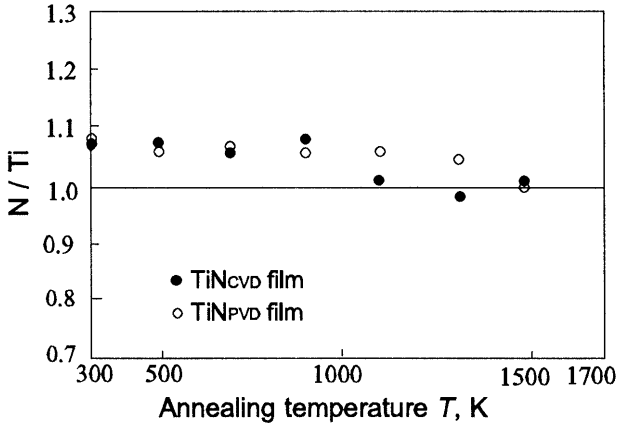

Fig.8. Changes in N/Ti ratio of the TiN_{CVD} and the TiN_{PVD} films with annealing treatments.

1.00 after annealing at 1473 K. As a result, in the case of the TiN_{CVD} films, as the Ti-N composition did not change after annealing below 1073 K, residual stress in the TiN_{CVD} films did not change after annealing below 1073 K. On the other hand, the decrease of residual stresses in the TiN_{PVD} films after annealing below 1073 K was attributed to the relaxation of intrinsic stress generated by an ion bombardment during the depositing process, because the Ti-N composition in the TiN_{PVD} films did not change after annealing below 1073K.

Compressive residual stresses in both TiN_{CVD} and TiN_{PVD} films increased by annealing above 1073 K. These stresses are nearly equal to the thermal residual stresses but the slight difference between them increased with increasing annealing temperatures. This difference may have been caused by stress relaxation during annealing as a result of plastic deformation in the substrate near the interface and the change in Ti-N composition.

5. CONCLUSIONS

Residual stresses in the TiN_{CVD} were measured by the X-ray two-exposure method. We investigated the residual stresses, Ti-N composition in the TiN film, and morphology of the film surface.

The TiN_{CVD} film has a structure with very high {100} orientation and compressive residual stress. The integrated intensity and FWHM did not change after annealing at temperatures below 1073 K but a large decrease in the integrated intensity and a large increase in the FWHM were observed after annealing at 1273 K. Compressive residual stresses in the TiN_{PVD} decreased with increasing annealing temperatures before reaching the minimum value at 1073 K. Residual stresses in the TiN_{CVD} films did not change after annealing at temperatures below 1073 K. After annealing above 1073 K,

residual stresses in the TiN_{CVD} and also in the TiN_{PVD} films began to increase to the compressive side along with the thermal residual stress but some differences existed between the measured stress and the thermal residual stress. Although the surface of the TiN_{CVD} films showed no significant change by annealing below 873 K, recrystallized TiN grains appeared on the surface when the specimen was annealed above 1073 K, which is higher than the depositing temperature (973 K). The ratio of N/Ti (TiN_{CVD} and TiN_{PVD} films) did not change by annealing below 1073 K but decreased to 1.00 after annealing above 1073 K.

REFERENCES

1. A. J. Perry, M. Jagner, W. D. Sproul and P. J. Rudnich, Surf. and Coat. Technol., **42** (1990) 49.
2. M. K. Hobbs, R. G. Cooke, B. Harris and H. Reiter, British Ceram. Proc., **39** (1989) 119.
3. G. C. Chang and W. Phucharoen, Surf. and Coat. Technol., **32** (1987) 307.
4. J. A. Sue, Surf. and Coat. Technol., **54-55** (1992) 154.
5. S. J. Bull, A. M. Jones and A. R. McCabe, Surf. and Coat. Technol., **54-55** (1992) 173.
6. T. Matsue, T. Hanabusa and Y. Ikeuchi, Thin Solid Films, **281-282** (1996) 344.
7. B. D. Cullity, Elements of X-Ray Diffraction, Addison-Wesley Co. Inc., Massachusetts (1978) p. 75.
8. W.G. Sloof, B.J. Kooi, R. Delhez, Th.H.de Keijser, and E.J.Mittemeijer, J.Mater. Res., **11** (1996) 1440.